Published as: *Nat Commun*. 2013 ; 4: 2332–2332.

Axonal and subcellular labeling using modified rabies viral vectors

Ian R. Wickersham, **Heather A. Sullivan**, and **H. Sebastian Seung**
Massachusetts Institute of Technology, Department of Brain & Cognitive Sciences, 43 Vassar St, Cambridge, MA 02139

Abstract

An important aspect of any neural circuit is the placement of its output synapses, at levels ranging from macroscopic to subcellular. The many new molecular tools for locating and manipulating synapses are limited by the viral vectors available for delivering them. Adeno-associated viruses are the best current means of labeling and manipulating axons and synapses, but they have never expressed more than one transgene highly enough to label fine axonal structure while also labeling or perturbing synapses. Their slow expression also makes them incompatible with retrograde and transsynaptic vectors, preventing powerful combinatorial experiments. Here we show that deletion-mutant rabies virus can be specifically targeted to cells local to an injection site, brightly labeling axons even when coexpressing two other transgenes. We demonstrate several novel capabilities: simultaneously labeling axons and presynaptic terminals, labeling both dendrites and postsynaptic densities, and simultaneously labeling a region's inputs and outputs using coinjected vectors.

INTRODUCTION

Understanding the role of any circuit within the brain requires knowledge of where else in the nervous system it sends its output. Because the major output pathways of almost all neurons are their axons, this is most straightforwardly achieved by imaging either the axons themselves or the synapses they form. Tools for "anterograde tracing", or labeling the axons that emanate from some site of interest, date back many decades [1], and the ongoing development of molecular biological tools is allowing the mapping and manipulation of

Corresponding author: IRW (wickersham@mit.edu).

AUTHOR CONTRIBUTIONS
IRW designed viral vectors and performed experiments. HAS cloned and produced viral vectors and assisted with histology. IRW and HSS designed experiments and wrote the manuscript.

COMPETING FINANCIAL INTERESTS
None.

ACCESSION CODES
Complete sequences of the genome plasmids for all vectors described in this manuscript have been deposited in the Genbank nucleotide database under accession codes 1642195, 1642209, 1642210, 1642211, 1642212, 1642213, 1642214, 1642215, 1642216, 1642217, 1642218, and 1642219.

synapses in much greater detail[2–9]. However, the viral vectors that have so far been available for delivering these molecular tools to axons and synapses have significant limitations.

The most prominent limitation of available “anterograde” (i.e., infecting cell bodies and delivering transgene products to axons) vectors is their inability to provide high-level expression of more than a single transgene[3, 9, 10]. Although multiple transgenes can of course be included in an adeno-associated virus (AAV), for example, to our knowledge there is no published example of any polycistronic viral vector that has simultaneously expressed any other transgene in combination with a cytoplasmic fluorophore expressed at levels high enough to allow clear visualization and reconstruction of axonal morphology. A recent such attempt illustrates the point: an AAV designed to express cytoplasmic mCherry along with a synaptobrevin-EGFP fusion resulted in cytoplasmic labeling only of the thickest axons, not the fine processes that are necessary, for example, to identify the cell bodies of origin of particular labeled synapses[11]. This inability of AAV to express multiple transgenes at high levels has prevented simple but powerful experiments such as simultaneously labeling synaptic locations and detailed axonal structure, or combining optogenetic confirmation of synaptic contacts with detailed reconstruction of axonal and dendritic architecture.

The timescales of existing anterograde vectors are also problematic. The viral species typically used for labeling axons require weeks or even months for adequate expression[3, 9, 11], while the few published alternatives with faster expression are so toxic that infected neurons sicken and die within 2–3 days[12, 13]. It would therefore be difficult to combine any of these vectors with those that allow gene delivery by two other routes of equally great importance: retrograde (in which genes are delivered to projection neurons through their axons projecting to a remote injection site) and transsynaptic (in which a viral vector spreads to the target neurons from neurons in synaptic contact with them). This is because rabies viral (RV) vectors, which are the best current means of both transsynaptic and retrograde gene delivery[14–23], have a working window that falls in the large gap between the very slow and very fast/toxic ranges of the available anterograde vectors. The lack of compatible anterograde and retrograde or transsynaptic vectors has prevented powerful combinatorial experiments, such as optically stimulating incoming anterogradely-targeted axons while imaging the resulting postsynaptic activity in retrogradely-targeted dendrites, with cytoplasmic fluorophores allowing imaging and 3D reconstruction of these neurites. What is needed is an anterograde vector that, first, allows high-level expression of multiple transgenes and, second, does so on a timescale that matches that of retrograde and transsynaptic vectors.

Here we show that deletion-mutant rabies virus (RV), which is ordinarily very efficient at retrogradely infecting distant neurons projecting to an injection site, can be transformed into a vector that specifically infects cells local to an injection site, simply by packaging it with the envelope protein of a different virus. This repackaging leaves intact its signature rapid, high and stereotyped transgene expression, so that axons can be brightly labeled with soluble fluorescent proteins, making them clearly individually resolvable. We also show that multiple transgenes can be incorporated into the RV genome with stereotyped expression levels that can be chosen based on the needs of the experiment., Single viral vectors can therefore be used to label multiple subcellular compartments, as in the example shown here

of labeling both dendrites and postsynaptic densities of retrogradely targeted neurons, which has never before been demonstrated. We combine the above characteristics to demonstrate bright, multicolor fluorescent anterograde labeling of neurons' axons and presynaptic terminals (which has itself never before been achieved) in addition to expression from the same viral vector of a third transgene, in this case used to label the neurons' nuclei in a third color. Because the timescale of expression from this anterograde version of RV matches those of the previously published retrograde and transsynaptic versions, the different vectors can be used in combination within the same subject for simultaneous gene delivery to different neuronal populations by different routes. This includes, as we show here, simultaneous tracing, in different colors, of both outputs and inputs of a region of interest by coinjecting anterograde and retrograde vectors.

RESULTS

Packaging RV with VSVG abolishes retrograde infectivity

We first investigated whether packaging RV vectors with the envelope glycoprotein of vesicular stomatitis virus (VSVG) would eliminate their usually marked propensity for retrogradely infecting remote neurons and instead target their infectivity to cells local to the injection site. This expectation seemed reasonable, because lentiviral vectors that are packaged with VSVG efficiently infect local neurons and glia but do not infect retrogradely when injected into the nervous system, while those that are instead packaged with the rabies virus envelope glycoprotein (RVG) infect retrogradely with efficiency comparable to that of rabies virus[14, 24] (albeit with far lower expression levels). We generated a VSVG-enveloped rabies viral vector encoding enhanced green fluorescent protein (EGFP)[25] by growing the previously described RV-4GFP[26] in cells expressing a fusion protein comprising the extracellular and transmembrane domains of VSVG (Indiana strain) and the cytoplasmic domain of RVG[27]; such substitution of the native RVG cytoplasmic tail increases the efficiency of incorporation into the envelopes of RV virions while preserving the tropism of the exogenous glycoprotein[15, 28, 29].

We equalized the titers of the VSVG-enveloped and RVG-enveloped preparations of RV-4GFP and injected equal volumes (20 nl) into the primary somatosensory cortex of different mice. Figure 1 depicts the results. As described previously[14], the RV enveloped with its native glycoprotein (schematically depicted in figure 1A) retrogradely infected neurons spread widely throughout the brain. At the injection site in cortex (figure 1B), labeled neurons were found diffusely, with distribution extending laterally from the injection site in layer 5 (the location of which is indicated by the presence of fluorescent glia) and a striking blade of labeled neurons in layer 2/3, consistent with the known projection from this layer to layer 5[30]. In thalamus, retrogradely infected relay neurons were found in the somatosensory nuclei (figure 1C), with most found in the ventral posteromedial nucleus (VPM, primary somatosensory nucleus) and smaller numbers in the posterior nucleus (Po, secondary somatosensory nucleus).

In sharp contrast, infection by the RV enveloped with the VSV glycoprotein (figure 1D–F) was restricted to a tight cluster of cells at the injection site (figure 1E). As seen in figure 1B and 1E, injection of the VSVG-enveloped vector resulted in far denser labeling of neurons at

the injection site than did injection of the RVG-enveloped version. This is presumably because the neurons infected by the VSVG-enveloped vector were almost entirely restricted to the injection site, whereas a large proportion of the neurons infected by the RVG-enveloped vector (which was matched in titer and injection volume) were remote projection neurons infected through their axon terminals at the injection site. There were no retrogradely infected cells in thalamus (figure 1F), only dense arbors of GFP-filled axons in both VPM and Po, matching the locations of retrogradely labeled relay neurons in the previous case. Supplementary Figure S1 shows close-ups of these anterogradely labeled axons, with very different morphologies of axons and terminals seen in the projections to the two different thalamic nuclei. Neurons retrogradely labeled by the VSVG-enveloped RV were very rarely seen (one found in superficial layer 2 of ipsilateral sensorimotor cortex 1.5 mm anterior to the injection site is shown in Supplementary Figure S2). However, this residual retrograde infectivity (which is also seen with AAV[31–33]) was not a major feature, with never more than two labeled neurons found in contralateral cortex, and none found in thalamus, in any animal.

Expression level depends on location in the RV genome

Next we quantified the expression levels of transgenes located at different loci within the RV genome, in order to better inform decisions of vector design for experiments requiring expression of multiple transgenes. We expected the expression levels of transgenes to depend on their locations in the viral genome, because the expression levels of the five endogenous rabies viral genes have been shown to decrease monotonically with increasing distance from the start (3' end) of the negative-strand RNA genome[34]. All previously published G-deleted rabies viral vectors contained one or two transgenes located in the position of the deleted glycoprotein gene between the viral matrix and polymerase genes[14, 26, 35–37]. We have now inserted an additional transgene locus at the start of the viral genome, immediately following the leader sequence and before the viral nucleoprotein gene. We expected that this would result in the highest possible transgene expression in addition to allowing the inclusion of a third transgene in a single vector.

We constructed an array of rabies viral vectors to compare the expression levels of transgenes located in these three positions. These vectors constituted a complete set, with all possible combinations of either zero or one transgene at the genome start, and zero, one or two transgenes in the place of G, with EGFP appearing as one of the transgenes in each possible position and with other transgenes included as placeholders as required (Figure 2a). We infected wells of HEK 293T cells with equal amounts of these vectors and quantified the intensity of the resulting fluorescence by flow cytometry (sample fluorescence histograms are shown in Supplementary Figure S3). As predicted, the expression from the various vectors was at stereotyped and distinct levels, with intensity decreasing with distance from the genome start. EGFP was expressed from the leader-proximal locus at a much higher level than from the previously used loci in the position of the deleted G: fluorescence resulting from the highest-expressing vector (vector iv in figure 2a) was 2.4-fold higher than that resulting from the single-gene version (vector i, previously described[26]), and 2.7-fold and 2.9-fold higher than the two versions with two transgenes only in the G locus (vectors ii and iii), as in previously published vectors[37]. Furthermore, addition of the new leader-

proximal locus decreased the expression level of genes (either one or two) in the original G locus, by 30% in the case of a single gene (vector vii vs. vector i) and 29% and 22% in the two-gene cases (vector viii vs. vector ii, and vector ix vs. vector iii). All these differences were highly significant (pairwise two-tailed t-tests, $P<0.0001$). Supplementary Table S1 contains the brightness means, standard deviations, numbers of fluorescent cells, standard errors of the means, t values, and degrees of freedom for all of the above comparisons.

Labelling both dendrites and postsynaptic densities

We took advantage of this ability to express multiple transgenes at defined and stereotyped levels to engineer vectors to simultaneously label different subcellular compartments of neurons. As an example, we constructed a genome with the sequence encoding mOrange2[38] in the leader-proximal locus and a gene encoding a fusion protein of PSD-95[39] and EGFP in the G locus and packaged this genome with the native RV G for retrograde delivery. Figure 2b–g depicts the apical dendrites of a layer 5 barrel cortical pyramidal cell retrogradely infected from an injection in the somatosensory thalamus. The vector brightly labels the detailed structure of dendrites with the cytoplasmically-soluble mOrange2, while the PSD-95-EGFP fusion results in punctate labeling along dendrites and prominent on dendritic spines.

Labelling of axons and synaptic terminals as well as nuclei

We combined these two abilities of RV - anterograde targeting, and expression of multiple transgenes at defined levels - to create an anterograde tracing tool for simultaneous multicolor fluorescent labeling of three separate subcellular compartments: first, axonal processes, to illuminate projection pathways and allow reconstruction of individual axons, second presynaptic terminals, to indicate the exact locations of synapses, and, third, the neurons' nuclei, for easily counting infected neurons to provide a "normalization factor" allowing quantitative comparison of the results of different injections[9]. We constructed a genome with the EGFP gene in the leader-proximal locus and two other transgenes in the G locus, the first encoding a nuclearly-localized version of the bright blue fluorophore mTagBFP[40] and the second encoding a fusion protein of synaptophysin[41] and the bright red fluorophore TagRFP-T[38] (genome v in Figure 2a). We packaged this genome with the VSV envelope protein for local infectivity and made 5-nanoliter injections into mouse somatosensory cortex. Figure 3 depicts the results.

At the injection site (panels A-D), a tightly focused cluster of neurons, mostly layer 6 pyramidal cells with apical dendrites ascending to and ramifying in layer 4, is brightly labeled with EGFP. Even at low magnification (panel A), axons can be clearly seen traversing en masse through the white matter and descending in distinct groups through the striatum. At higher magnification (25X, panels B-D), individual neurons are clearly resolvable, particularly in the blue channel in which nuclei are distinctly labeled. In this field, 71 BFP-labeled nuclei are resolvable, with all but 4 (94.4%) unambiguously colocalized with EGFP-labeled somata. High-power (100X, panels E-G) imaging of the somatosensory thalamus (VPM) reveals that the EGFP-labeled fine processes of axonal arbors are easily resolvable, with punctate red fluorescence from the synaptophysin-TagRFP-T fusion protein colocalized with varicosities on the axons.

Two-colour fluorescent labeling of inputs and outputs

We then examined whether the novel anterograde RV vector could be used in combination with the previously published retrograde version, and, specifically, whether it was possible to jointly trace both the inputs and the outputs of a brain region by injecting a mixture of two viral vectors. This represents a powerful combinatorial assay much more informative than separately labeling inputs and outputs in different animals, because it would allow determination of the precise spatial register of outgoing axons with the dendrites of neurons projecting to the injection site, in any of the many cases of reciprocal connections between nuclei within the brain. We injected into mouse somatosensory thalamus (ventral posteromedial nucleus) an equal mixture of two rabies viral vectors: one anterograde (VSVG-enveloped) and encoding mOrange2[38], the other retrograde (RVG-enveloped) and encoding mCherry[42]. The results are shown in figure 4. At the injection site in thalamus, many relay neurons, as well as glia, were brilliantly labeled with mOrange2 (Figure 4A & B). These neurons' axons heavily innervated primary somatosensory cortex (Figure 4D & E), running along the subcortical white matter before ascending through layers 6 and 5 and ramifying densely in layer 4 (Figure 4D & E). By contrast, the retrograde virus labeled few cell bodies, but many processes, at the thalamic injection site (Figure 4A & C). While some cells were coinfected by the two viruses (although some of the apparent mCherry fluorescence in thalamus may be due to spectral overlap from the intense mOrange2 expression in cell bodies and processes there), most were not. This is most obvious in cortex (Figure 4D–F), where the vast majority of mOrange2-labeled thalamocortical axons did not express mCherry. However, many layer 6 pyramidal cells were retrogradely labeled with mCherry, in precise topographic register with the mOrange2-labeled thalamocortical projection. These cells' apical dendrites ascended to layer 4 and terminated there, in the region of densest thalamocortical axonal ramification.

DISCUSSION

We have shown here that packaging G-deleted RV with the VSV envelope protein, instead of the native RV one, almost completely removes its otherwise notable ability to infect retrogradely and causes it instead to efficiently infect local neurons. Because the tropism of VSVG-enveloped RV is determined by the VSV envelope protein itself, it can be expected to be pantropic and, furthermore, to work in a wide variety of taxa, including primates[43], birds[44], and insects[45]. Despite its redirected tropism, the VSVG-enveloped version of RV retains the high and rapid transgene expression characteristic of the original, because the vectors are identical apart from their means of reaching the cytoplasm. For the same reason, we expect that the time courses of transgene expression levels and host cell toxicity are also similar.

Here we have illustrated RV vectors' ability to coexpress multiple transgenes at stereotyped but differing levels (Figure 2a) by constructing a vector to coexpress cytoplasmic mOrange2 and a PSD-95-EGFP fusion protein (Figure 2b–g). This constitutes the first published case of simultaneously labeling both dendrites and the postsynaptic sites on them by means of any retrograde vector. We expect vectors of this kind to be very useful tools in their own right for a number of important applications, such as rapid quantification of synaptic scaling

along dendritic branches of single neurons, a critical determinant of the integrative properties of dendritic arbors[46]. It is entirely possible that the expression levels of synaptic fusion proteins are excessive when these transgenes are located in the original G locus, as in the example vectors we have presented here. Overexpression of PSD-95, in particular, can be perturbative[47], although, to the extent to which we have quantified synaptic density here (counting the PSD-95-EGFP-labeled puncta in Figure S4), it appears in line with other published data[48–50]. Similarly, the 2.4-fold increase of EGFP expression resulting from placement of the new locus in the promoter-proximal position (where the EGFP gene also has been positioned in VSV vectors[12] and, unsuccessfully, in replication-competent RV[51]) may be overkill, because EGFP expressed from the G locus is already sufficient for labeling fine axonal processes[14, 16], and even EGFP can be toxic at high levels[52]. It may therefore be desirable to design future vectors for lower transgene expression levels. We have shown here that multiple transgenes placed in the G locus are expressed at levels only slightly lower than those of single-transgene versions. Expression could be lowered further by straightforward means. Just as, as we have shown here, expression can be increased by moving transgenes closer to the start of the RV genome, it could as easily be decreased simply by moving them farther away, with loci added at the end of the genome (after the viral polymerase gene) expected to result in expression considerably lower than from any of the loci used here or in any previous deletion-mutant RV vectors. Furthermore, it should be possible to engineer arbitrarily low - but still stereotyped - expression levels by the insertion of multiple such loci (even empty ones consisting only of transcriptional start and stop signals, included only as spacers to decrease expression of downstream transgenes) at the 5’ end of the viral genome.

Our use of a VSVG-enveloped RV vector for multicolor labeling of axons, synaptic terminals and nuclei of neurons at an injection site (Figure 3) is innovative in several ways. First, simultaneously labeling axonal fine structure and synaptic terminals using a single viral vector has not previously been demonstrated, despite attempts to do so[11]. We have not only achieved this but also included a third transgene, in this case for labeling nuclei as well. Second, to our knowledge, this is the first published demonstration that three transgenes can be expressed from a single RV vector. This allows great flexibility in experimental design. Here we have used this option of a third transgene simply for expressing a third, nuclearly-localized fluorophore, which would be useful in cases in which rapid counting of labeled neurons is needed for comparison of different injections[9]. Alternatively, this third transgene locus could be used instead for expression of channelrhodopsin, a calcium indicator, or indeed any other transgene[20, 21, 37].

Although there may be as-yet-unclear practical limits on the lengths of rabies viral vector genomes, there appears to be no hard constraint. The largest one that we have constructed for this work (genome v in Figure 2 and used for the injections shown in Figure 3) contains transgenes totaling 3228 bases (720, 813 and 1695 bases for EGFP, nuclearly-localized BFP, and synaptophysin-TagRFP-T, respectively) for a total length of 13,353 bases (versus 11928 bases for the wild-type SAD B19 genome[53]). However, RV vectors containing two transgenes totaling up to 6.5 kb have previously been constructed, even without deleting the glycoprotein gene as we have done with all of the vectors presented here[54].

Simultaneously labeling the axons proceeding from a region of interest while also labeling the remote neurons sending projections to it, as we have demonstrated here, has not previously been achieved with any combination of viral vectors. In theory, this could be possible using other viral species, such an AAV for anterogradely labeling axons coinjected with an HSV vector for retrogradely labeling projection neurons[55]. Assuming expression levels from such retrograde infection with an HSV are high enough for clear labeling of fine dendritic processes, this would presumably have the advantage of lower toxicity, which would be very useful for long-term studies. However, using RV vectors has two major advantages. The first and most obvious is the ability to express multiple transgenes at high levels, as discussed above. The second, however, is the notable lack of coinfection seen when the two RV variants are coinjected (Figure 4), with the VSVG-enveloped anterograde virus evidently outcompeting the RVG-enveloped retrograde virus for infection of cells local to the injection site. This seems to be an example of the “superinfection interference” that is a prominent feature of (even intracellularly) replication-competent viruses and which is seen also with intact RV[51]. Often a nuisance (hindering double-labeling studies, for example), in this case it allows not just simultaneous tracing of both outputs and inputs of a region of interest, but also largely non-overlapping expression of different transgenes in the two populations, so that the thalamocortical axons (panel E) do not express the transgene labeling the dendrites of the corticothalamic cells (panel F) and vice versa. This therefore would allow many other powerful combinatorial assays of reciprocal connections, such as including synaptic markers similar to those used in figures 2 and 3 for identification of putative synaptic contacts between the labeled axons and dendrites, or all-optical interrogation of the thalamocorticothalamic circuit by expressing opsins in thalamocortical axons and expressing activity indicators in corticothalamic dendrites.

We have here demonstrated that, in addition to the previously described retrograde[14], transsynaptic[15], and genetic[15, 56] delivery routes, rabies viral vectors can also be engineered to target neurons by a fourth route: anterograde delivery of transgene products to axons (see Figure 5). With the additional ability to express multiple transgenes in each of the vectors used to target distinct neuronal populations by any of these four routes, this opens the door to focal identification and interrogation of synapses throughout the brain. One possible paradigm would be to express GRASP components[4, 6, 8] - the use of which has so far been restricted to application-specific transgenic and knock-in animals - in a wide range of putatively presynaptic and postsynaptic populations, e.g., by anterograde and retrograde targeting, respectively. Alternatively, one could anterogradely label several separate inputs to a region by injecting different vectors in the nuclei that give rise to them, causing expression of different opsins in these various groups of axons, allowing their independent optical activation and determination of their effect on postsynaptic neuronal populations targeted retrogradely or transsynaptically for expression of calcium or voltage indicators, with coexpressed cytoplasmic fluorophores allowing 3-dimensional reconstruction of all the neurites involved. Because as demonstrated here, these vectors can incorporate even three transgenes, the above paradigms could furthermore be combined to allow structural and functional interrogation of exactly the same circuits. These combinatorial possibilities are limited only by the spectral separation of fluorophores, activators and indicators, a barrier

that is rapidly eroding with the ongoing development and refinement of these molecular tools.

METHODS

Cloning

All viral genome plasmids were derived from cSPBN[57] (itself derived from the SAD B19 genome plasmid pSAD L16[58]), with the glycoprotein gene deleted in all cases. For some vectors (such as the bottom six genomes depicted in figure 3a), an additional open reading frame was inserted between the viral leader sequence and the nucleoprotein gene. All vectors had either one or two transgenes cloned into the G locus, with the exception of RV-1E (sixth genome from top in figure 3a), for which the G locus (including start and stop sequences) was deleted entirely. The nuclearly-localized blue fluorescent protein gene was constructed by cloning the mTagBFP[40] gene in frame with the nuclear localization signal (SV40 large T antigen triple tandem repeat) from pEYFP-Nuc (Clontech, Mountain View, CA). The fusion protein of PSD-95 with EGFP[25] was constructed by cloning the rat PSD-95 gene[59] in frame with that of EGFP. The fusion protein of synaptophysin with TagRFP-T[38] was constructed by de novo synthesis of the mouse synaptophysin gene[41] (GenBank accession number X95818) in frame with that of TagRFP-T. Gene synthesis and many cloning steps were performed by Epoch Life Science, Inc. (Missouri City, TX).

Vector production

Vector production subsequent to cloning was performed by cotransfection of viral genome and helper plasmids followed by amplification by passaging in complementing cells[26] but using the BSR-VSV-RV-G cell line[27] instead of the BHK-B19G2 line[26] for the anterograde vectors. For vectors with a transgene preceding the nucleoprotein gene (e.g. the last six genomes depicted in Figure 3a), supernatants were collected for one additional day (i.e. at 48, 72, and 96 hours following infection). Vectors were concentrated and purified by ultracentrifugation (2 h at 51,000g, Thermo Surespin 630 rotor) of supernatants, with virus extracted from the interface of 20% and 60% sucrose solutions (w/v in Dulbecco's phosphate-buffered saline DPBS), diluted in DPBS and pelleted by a second round of ultracentrifugation to remove sucrose, resuspended in DPBS and stored in 5–20 ul aliquots at −80C.

Titer determination and flow cytometric analysis

HEK-293T cells (ATCC # CRL-11268) in 24 well plates were infected with serial dilutions[26] with medium changed 20 hours after infection and cells resuspended in 1% paraformaldehyde after three days. Suspensions were analyzed on a BD LSR II flow cytometer (BD Biosciences, San Jose, CA), with fluorescent cells' brightness means and variances calculated using BD FACSDiva software. For t-tests, sample sizes for the nine groups were determined by the fraction of the total number of analyzed cells (30,000 in each group) that was positive for EGFP fluorescence; these sample sizes were: i (4GFP) 2553, ii (4E5S) 1893, iii (4nB5E) 2209, iv (1E5S) 1732, v (1E5nB6SR) 1660, vi (1E) 1561, vii (1mC5E) 1550, viii (1mC5E6S) 2820, ix (1mC5nB6E) 2873.

Stereotaxic injections

All work with animals was approved by the MIT Committee for Animal Care. Vectors were injected into either primary somatosensory cortex (−0.58 AP, +3.0 LM, −1.75 DV, mm relative to bregma) or ventral posteriomedial nucleus (−1.82 AP, +1.75 LM, −3.5 DV) of anesthetized adult male C57BL/6J mice (Jackson Laboratory, Bar Harbor, ME) using a stereotaxic instrument (Stoelting Co., Wood Dale, IL) and an injection mechanism consisting of a hydraulic manipulator (MO-10; Narishige Group, Tokyo, Japan) with headstage coupled via a custom adaptor to a wire plunger advanced through pulled glass capillaries (Wiretrol II, Drummond) backfilled with mineral oil and front-filled with vector stock solution. For the matched injections of RVG- and VSVG-enveloped vectors (figure 1), titers of both stocks were normalized to 2.0E10 i.u./ml, with 20 nanoliters (4E5 i.u.) of either stock injected per animal (n=5 in each case). For retrograde bicolor labeling of dendrites and postsynaptic densities (figure 2), 200 nanoliters of virus (5.4E8 i.u./ml, 1.1E5 i.u. total) was injected into VPM (n=1). For anterograde tricolor labeling of axons, nuclei and presynaptic terminals (figure 3), 5 nanoliters of virus (8.6E9 i.u./ml, 4.3E4 i.u. total) was injected into cortex (n=2). For the joint injections of anterograde and retrograde vectors (figure 4), a mixture containing 8.0E8 i.u./ml of each was prepared and 50 nanoliters (4.0E4 i.u. of each vector) injected per animal (n=2).

Histology and imaging

6–7 days following vector injection, mice were perfused transcardially with 4% paraformaldehyde in phosphate-buffered saline. Brains were postfixed in 4% paraformaldehyde overnight at 4°C and cut into 50 um coronal sections using a vibrating microtome (VF-700; Precisionary Instruments, San Jose, CA). Sections were mounted on Superfrost Plus slides (Fisher Scientific, Pittsburg, PA) with Prolong Gold Antifade mounting medium (Life Technologies, Grand Island, NY) and imaged on Olympus (Tokyo, Japan) FV1000 and Zeiss (Jena, Germany) LSM 710 confocal microscopes.

Supplementary Material

Refer to Web version on PubMed Central for supplementary material.

ACKNOWLEDGEMENTS

We thank Matthias Schnell for generously providing the BSR-VSV-RV-G cell line, Klaus Conzelmann for helpful discussions and ongoing generosity in granting requests for distribution of plasmids, Jerry Chen and Elly Nedivi for providing the PSD-95 gene, Nikki Watson and Wendy Salmon for assistance with confocal imaging, Carlos Lois for helpful discussions, sharing equipment and assistance with setting up the custom virus injection system, Susumu Tonegawa for sharing equipment and Partha Mitra for helpful discussions. Funding was provided by the Howard Hughes Medical Institute and the McGovern Institute Neurotechnology Program.

REFERENCES

1. Jones EG, Hartman BK. Recent advances in neuroanatomical methodology. Annual review of neuroscience. 1978; 1:215–296.
2. Chamberlin NL, Du B, de Lacalle S, Saper CB. Recombinant adeno-associated virus vector: use for transgene expression and anterograde tract tracing in the CNS. Brain research. 1998; 793:169–175. [PubMed: 9630611]

3. Grinevich V, Brecht M, Osten P. Monosynaptic pathway from rat vibrissa motor cortex to facial motor neurons revealed by lentivirus-based axonal tracing. The Journal of neuroscience : the official journal of the Society for Neuroscience. 2005; 25:8250–8258. [PubMed: 16148232]
4. Feinberg EH, et al. GFP Reconstitution Across Synaptic Partners (GRASP) defines cell contacts and synapses in living nervous systems. Neuron. 2008; 57:353–363. [PubMed: 18255029]
5. Petreanu L, Mao T, Sternson SM, Svoboda K. The subcellular organization of neocortical excitatory connections. Nature. 2009; 457:1142–1145. [PubMed: 19151697]
6. Kim J, et al. mGRASP enables mapping mammalian synaptic connectivity with light microscopy. Nature Methods. 2011
7. Shu X, et al. A genetically encoded tag for correlated light and electron microscopy of intact cells, tissues, and organisms. PLoS biology. 2011; 9:e1001041. [PubMed: 21483721]
8. Yamagata M, Sanes JR. Transgenic strategy for identifying synaptic connections in mice by fluorescence complementation (GRASP). Front Mol Neurosci. 2012; 5:18. [PubMed: 22355283]
9. Harris JA, Wook Oh S, Zeng H. Adeno-associated viral vectors for anterograde axonal tracing with fluorescent proteins in nontransgenic and cre driver mice. Curr Protoc Neurosci. 2012 Chapter 1, Unit 1 20 21-18.
10. Roberts TF, Klein ME, Kubke MF, Wild JM, Mooney R. Telencephalic neurons monosynaptically link brainstem and forebrain premotor networks necessary for song. The Journal of neuroscience : the official journal of the Society for Neuroscience. 2008; 28:3479–3489. [PubMed: 18367614]
11. Xu W, Sudhof TC. A neural circuit for memory specificity and generalization. Science. 2013; 339:1290–1295. [PubMed: 23493706]
12. van den Pol AN, et al. Viral strategies for studying the brain, including a replication-restricted self-amplifying delta-G vesicular stomatis virus that rapidly expresses transgenes in brain and can generate a multicolor golgi-like expression. J Comp Neurol. 2009; 516:456–481. [PubMed: 19672982]
13. Ghosh S, et al. Sensory maps in the olfactory cortex defined by long-range viral tracing of single neurons. Nature. 2011; 472:217–220. [PubMed: 21451523]
14. Wickersham IR, Finke S, Conzelmann KK, Callaway EM. Retrograde neuronal tracing with a deletion-mutant rabies virus. Nature Methods. 2007; 4:47–49. [PubMed: 17179932]
15. Wickersham IR, et al. Monosynaptic restriction of transsynaptic tracing from single, genetically targeted neurons. Neuron. 2007; 53:639–647. [PubMed: 17329205]
16. Larsen DD, Wickersham IR, Callaway EM. Retrograde tracing with recombinant rabies virus reveals correlations between projection targets and dendritic architecture in layer 5 of mouse barrel cortex. Frontiers in neural circuits. 2007; 1:5. [PubMed: 18946547]
17. Wall NR, Wickersham IR, Cetin A, De La Parra M, Callaway EM. Monosynaptic circuit tracing in vivo through Cre-dependent targeting and complementation of modified rabies virus. Proceedings of the National Academy of Sciences of the United States of America. 2010
18. Weible AP, et al. Transgenic targeting of recombinant rabies virus reveals monosynaptic connectivity of specific neurons. The Journal of neuroscience : the official journal of the Society for Neuroscience. 2010; 30:16509–16513. [PubMed: 21147990]
19. Miyamichi K, et al. Cortical representations of olfactory input by trans-synaptic tracing. Nature. 2011; 472:191–196. [PubMed: 21179085]
20. Kiritani T, Wickersham IR, Seung HS, Shepherd GM. Hierarchical connectivity and connection-specific dynamics in the corticospinal-corticostriatal microcircuit in mouse motor cortex. The Journal of neuroscience : the official journal of the Society for Neuroscience. 2012; 32:4992–5001. [PubMed: 22492054]
21. Apicella AJ, Wickersham IR, Seung HS, Shepherd GM. Laminarly orthogonal excitation of fast-spiking and low-threshold-spiking interneurons in mouse motor cortex. The Journal of neuroscience : the official journal of the Society for Neuroscience. 2012; 32:7021–7033. [PubMed: 22593070]
22. Watabe-Uchida M, Zhu L, Ogawa SK, Vamanrao A, Uchida N. Whole-brain mapping of direct inputs to midbrain dopamine neurons. Neuron. 2012; 74:858–873. [PubMed: 22681690]
23. Lammel S, et al. Input-specific control of reward and aversion in the ventral tegmental area. Nature. 2012; 491:212–217. [PubMed: 23064228]

24. Mazarakis ND, et al. Rabies virus glycoprotein pseudotyping of lentiviral vectors enables retrograde axonal transport and access to the nervous system after peripheral delivery. Hum Mol Genet. 2001; 10:2109–2121. [PubMed: 11590128]
25. Thastrup O, Tullin S, Poulsen LK, Bjorn SP. 2001
26. Wickersham IR, Sullivan HA, Seung HS. Production of glycoprotein-deleted rabies viruses for monosynaptic tracing and high-level gene expression in neurons. Nature protocols. 2010; 5:595–606. [PubMed: 20203674]
27. Gomme EA, Faul EJ, Flomenberg P, McGettigan JP, Schnell MJ. Characterization of a single-cycle rabies virus-based vaccine vector. Journal of virology. 2010; 84:2820–2831. [PubMed: 20053743]
28. Mebatsion T, Conzelmann KK. Specific infection of CD4+ target cells by recombinant rabies virus pseudotypes carrying the HIV-1 envelope spike protein. Proc Natl Acad Sci U S A. 1996; 93:11366–11370. [PubMed: 8876141]
29. Mebatsion T, Finke S, Weiland F, Conzelmann KK. A CXCR4/CD4 pseudotype rhabdovirus that selectively infects HIV-1 envelope protein-expressing cells. Cell. 1997; 90:841–847. [PubMed: 9298896]
30. Lefort S, Tomm C, Floyd Sarria JC, Petersen CC. The excitatory neuronal network of the C2 barrel column in mouse primary somatosensory cortex. Neuron. 2009; 61:301–316. [PubMed: 19186171]
31. Passini MA, et al. AAV vector-mediated correction of brain pathology in a mouse model of Niemann-Pick A disease. Molecular therapy : the journal of the American Society of Gene Therapy. 2005; 11:754–762. [PubMed: 15851014]
32. Masamizu Y, et al. Local and retrograde gene transfer into primate neuronal pathways via adeno-associated virus serotype 8 and 9. Neuroscience. 2011; 193:249–258. [PubMed: 21782903]
33. Kornum BR, et al. Adeno-associated viral vector serotypes 1 and 5 targeted to the neonatal rat and pig striatum induce widespread transgene expression in the forebrain. Exp Neurol. 2010; 222:70–85. [PubMed: 20025873]
34. Finke S, Cox JH, Conzelmann KK. Differential transcription attenuation of rabies virus genes by intergenic regions: generation of recombinant viruses overexpressing the polymerase gene. Journal of virology. 2000; 74:7261–7269. [PubMed: 10906180]
35. Foley HD, McGettigan JP, Siler CA, Dietzschold B, Schnell MJ. A recombinant rabies virus expressing vesicular stomatitis virus glycoprotein fails to protect against rabies virus infection. Proceedings of the National Academy of Sciences of the United States of America. 2000; 97:14680–14685. [PubMed: 11114165]
36. McKenna PM, et al. Highly attenuated rabies virus-based vaccine vectors expressing simian-human immunodeficiency virus89.6P Env and simian immunodeficiency virusmac239 Gag are safe in rhesus macaques and protect from an AIDS-like disease. The Journal of infectious diseases. 2007; 195:980–988. [PubMed: 17330788]
37. Osakada F, et al. New rabies virus variants for monitoring and manipulating activity and gene expression in defined neural circuits. Neuron. 2011; 71:617–631. [PubMed: 21867879]
38. Shaner NC, et al. Improving the photostability of bright monomeric orange and red fluorescent proteins. Nat Methods. 2008; 5:545–551. [PubMed: 18454154]
39. Hsueh YP, Sheng M. Requirement of N-terminal cysteines of PSD-95 for PSD-95 multimerization and ternary complex formation, but not for binding to potassium channel Kv1.4. The Journal of biological chemistry. 1999; 274:532–536. [PubMed: 9867876]
40. Subach OM, et al. Conversion of red fluorescent protein into a bright blue probe. Chem Biol. 2008; 15:1116–1124. [PubMed: 18940671]
41. Gaitanou M, Mamalaki A, Merkouri E, Matsas R. Purification and cDNA cloning of mouse BM89 antigen shows that it is identical with the synaptic vesicle protein synaptophysin. J Neurosci Res. 1997; 48:507–514. [PubMed: 9210520]
42. Shaner NC, et al. Improved monomeric red, orange and yellow fluorescent proteins derived from Discosoma sp. red fluorescent protein. Nat Biotechnol. 2004; 22:1567–1572. [PubMed: 15558047]
43. Kordower JH, et al. Neurodegeneration prevented by lentiviral vector delivery of GDNF in primate models of Parkinson's disease. Science. 2000; 290:767–773. [PubMed: 11052933]

44. Bauer EE, et al. A synaptic basis for auditory-vocal integration in the songbird. The Journal of neuroscience : the official journal of the Society for Neuroscience. 2008; 28:1509–1522. [PubMed: 18256272]
45. Shelly S, Lukinova N, Bambina S, Berman A, Cherry S. Autophagy is an essential component of Drosophila immunity against vesicular stomatitis virus. Immunity. 2009; 30:588–598. [PubMed: 19362021]
46. Katz Y, et al. Synapse distribution suggests a two-stage model of dendritic integration in CA1 pyramidal neurons. Neuron. 2009; 63:171–177. [PubMed: 19640476]
47. El-Husseini AE, Schnell E, Chetkovich DM, Nicoll RA, Bredt DS. PSD-95 involvement in maturation of excitatory synapses. Science. 2000; 290:1364–1368. [PubMed: 11082065]
48. Holtmaat AJ, et al. Transient and persistent dendritic spines in the neocortex in vivo. Neuron. 2005; 45:279–291. [PubMed: 15664179]
49. Stuss DP, Boyd JD, Levin DB, Delaney KR. MeCP2 mutation results in compartment-specific reductions in dendritic branching and spine density in layer 5 motor cortical neurons of YFP-H mice. PLoS One. 2012; 7:e31896. [PubMed: 22412847]
50. Ghosh A, et al. Heterogeneous spine loss in layer 5 cortical neurons after spinal cord injury. Cerebral cortex. 2012; 22:1309–1317. [PubMed: 21840844]
51. Ohara S, et al. Dual transneuronal tracing in the rat entorhinal-hippocampal circuit by intracerebral injection of recombinant rabies virus vectors. Frontiers in neuroanatomy. 2009; 3:1. [PubMed: 19169410]
52. Liu HS, Jan MS, Chou CK, Chen PH, Ke NJ. Is green fluorescent protein toxic to the living cells? Biochemical and biophysical research communications. 1999; 260:712–717. [PubMed: 10403831]
53. Conzelmann KK, Cox JH, Schneider LG, Thiel HJ. Molecular cloning and complete nucleotide sequence of the attenuated rabies virus SAD B19. Virology. 1990; 175:485–499. [PubMed: 2139267]
54. McGettigan JP, et al. Functional human immunodeficiency virus type 1 (HIV-1) Gag-Pol or HIV-1 Gag-Pol and env expressed from a single rhabdovirus-based vaccine vector genome. Journal of virology. 2003; 77:10889–10899. [PubMed: 14512539]
55. Lima SQ, Hromadka T, Znamenskiy P, Zador AM. PINP: a new method of tagging neuronal populations for identification during in vivo electrophysiological recording. PLoS One. 2009; 4:e6099. [PubMed: 19584920]
56. Choi J, Young JA, Callaway EM. Selective viral vector transduction of ErbB4 expressing cortical interneurons in vivo with a viral receptor-ligand bridge protein. Proceedings of the National Academy of Sciences of the United States of America. 2010; 107:16703–16708. [PubMed: 20823240]
57. McGettigan JP, et al. Functional human immunodeficiency virus type 1 (HIV-1) Gag-Pol or HIV-1 Gag-Pol and env expressed from a single rhabdovirus-based vaccine vector genome. J Virol. 2003; 77:10889–10899. [PubMed: 14512539]
58. Schnell MJ, Mebatsion T, Conzelmann KK. Infectious rabies viruses from cloned cDNA. Embo J. 1994; 13:4195–4203. [PubMed: 7925265]
59. Hsueh YP, Sheng M. Regulated expression and subcellular localization of syndecan heparan sulfate proteoglycans and the syndecan-binding protein CASK/LIN-2 during rat brain development. The Journal of neuroscience : the official journal of the Society for Neuroscience. 1999; 19:7415–7425. [PubMed: 10460248]
60. Franklin, KBJ., Paxinos, G. The mouse brain in stereotaxic coordinates. Edn. 3rd.. Boston: Elsevier/Academic Press, Amsterdam; 2008.

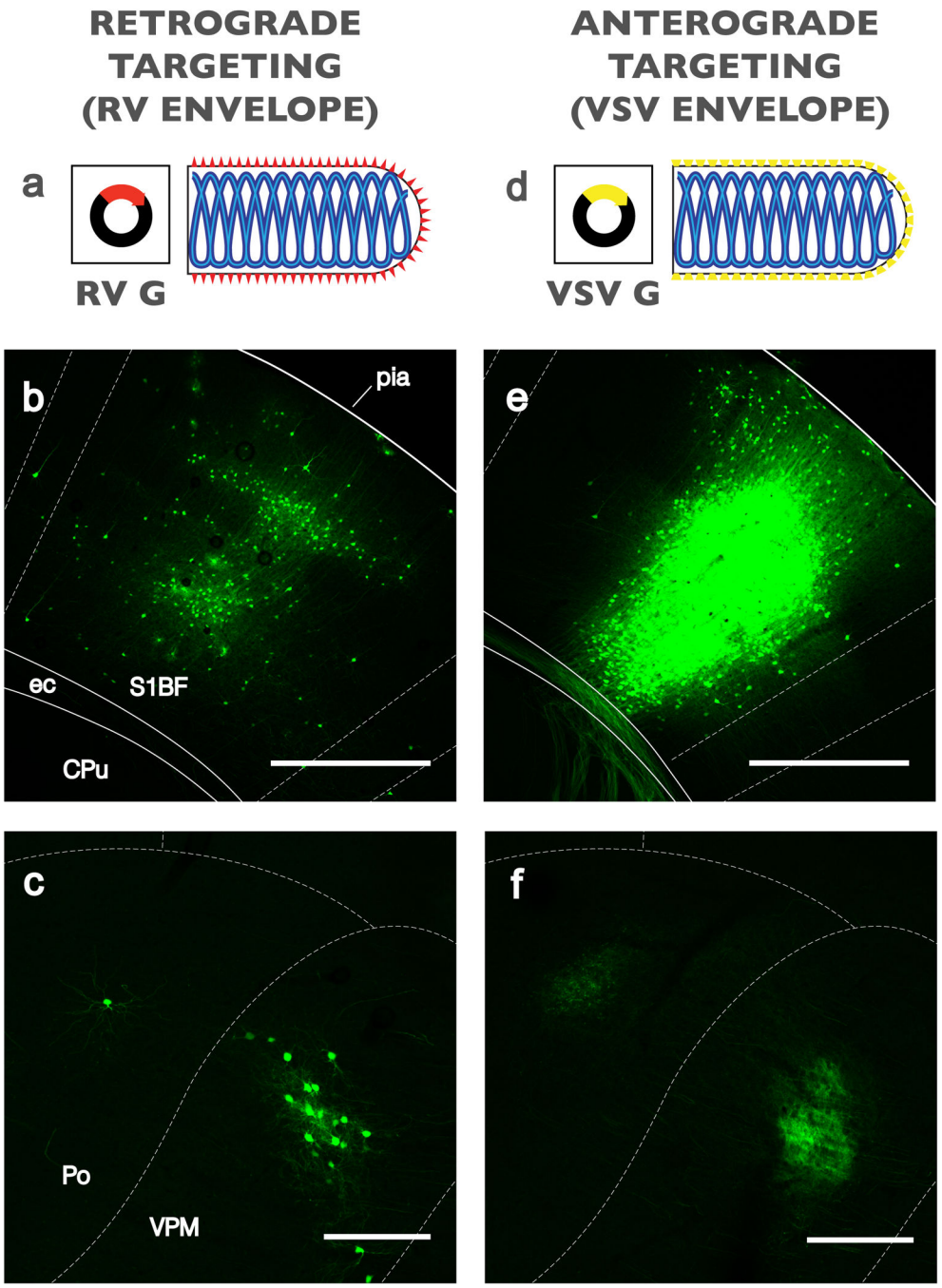

Fig. 1.

Packaging deletion-mutant RV with the VSV envelope protein abolishes retrograde infectivity. A) Schematic of packaging G-deleted RV with its own envelope protein for efficient infection of distant neurons projecting to an injection site, as described in Wickersham et al. ’07a. B) Injection site in mouse barrel cortex of RV-4GFP packaged with RV G. Many cortical neurons with cell bodies distant from the injection site are labeled. C) Numerous retrogradely infected cells are also present in the somatosensory thalamus (VPM and Po nuclei) of the same mouse. D) Schematic of packaging G-deleted RV with the VSV

envelope protein for local instead of retrograde infection. E) Injection site in mouse barrel cortex of RV-4GFP packaged with VSV G, with injection volume and viral titer equal to those of the injection depicted in panels B and C. Infected neurons are restricted to a tight cluster at the injection site, with bright GFP labeling of their axons. F) The somatosensory thalamus of the same animal contains dense arborizations of cortical axons in VPM and Po brightly labeled with GFP, but no retrogradely labeled cell bodies. Overlays indicating approximate structural boundaries are adapted from Franklin and Paxinos[60]. Abbreviations: S1BF = primary somatosensory cortex, barrel field; ec = external capsule; CPu = caudate putamen; Po = posterior thalamic nuclear group; VPM = ventral posteromedial thalamic nucleus. Scale bars: B & E 500 um, C & F 200 um.

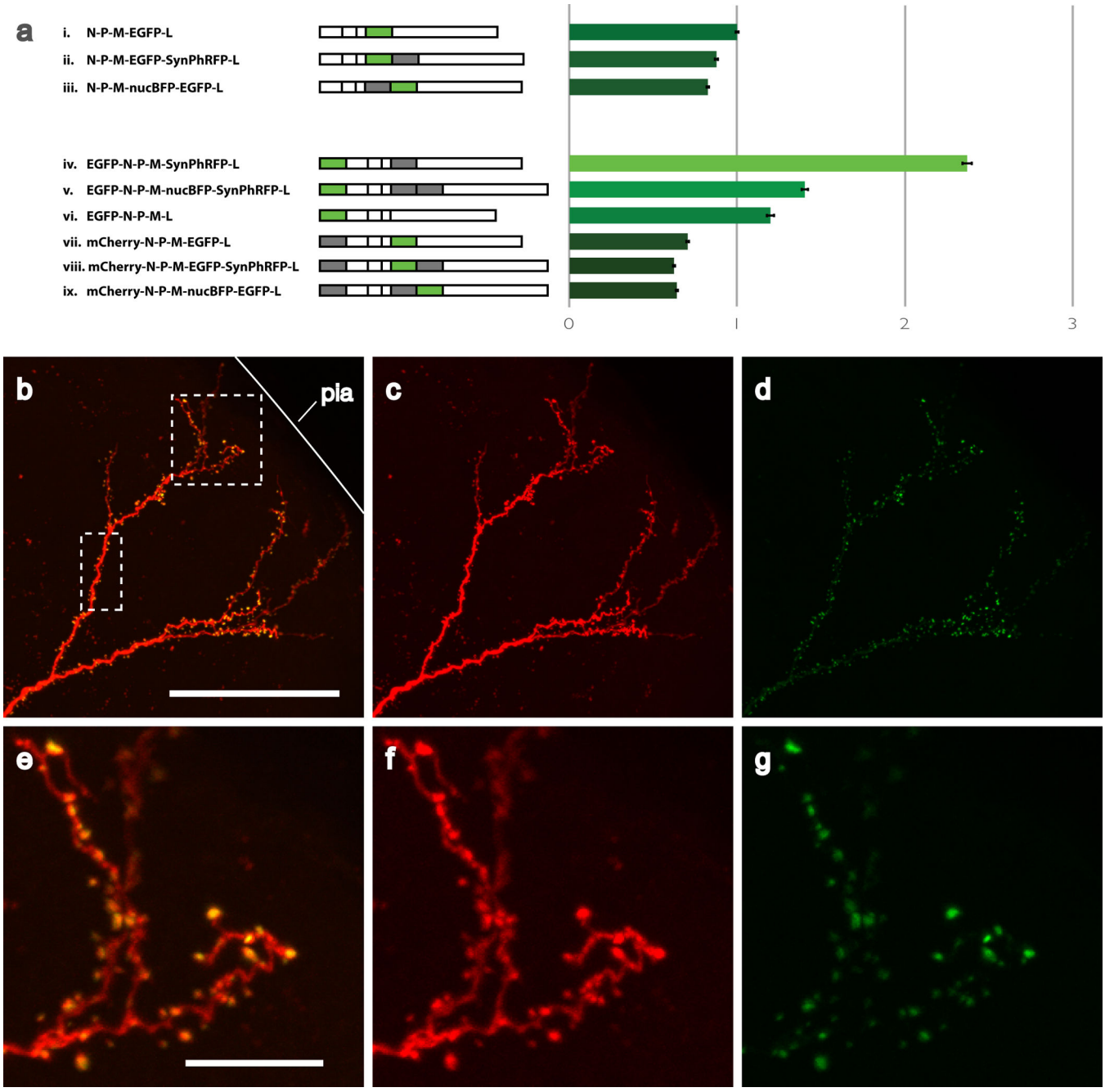

Fig. 2.

Expression of multiple transgenes from single vectors allows simultaneous labeling of neurites and synapses. A) Transgene location within the viral genome determines expression level, as determined by flow cytometric analysis of EGFP brightness. Two transgenes inserted in the G locus have only slightly lower expression than a single one. Addition of a transgene in the promoter-proximal locus prior to the first viral gene, with a second transgene in the original G locus, results in expression 2.4-fold higher than that of a single gene in the G locus. Error bars denote standard error of the mean (n=?). B–C) Two-color brightly fluorescent labeling of the apical dendrites and postsynaptic densities of a layer 5

cortical pyramidal cell. Cytoplasmic mOrange2 is expressed at a high level from the promoter-proximal locus; PSD-95-EGFP fusion is expressed at a lower level from the G locus. Solid line indicates approximate location of pia; dashed square indicates region enlarged in panels D–E; dashed rectangle indicates region enlarged in Supplementary Figure S4. D–E) Higher-resolution image of region enclosed by dashed square in panel B. EGFP puncta are located on dendritic spines. Scale bars: B–D 50 um, E–G 10 um.

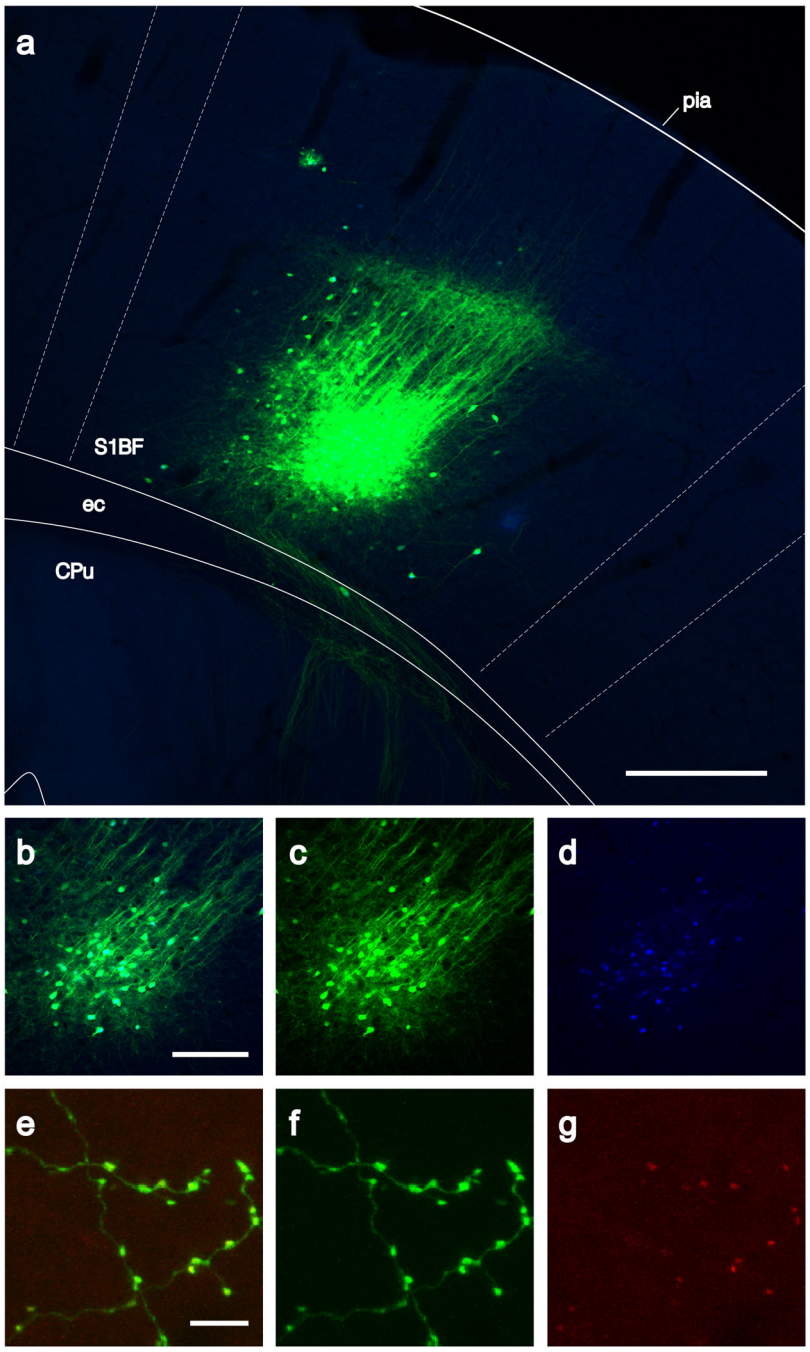

Fig. 3.

Simultaneous multicolor brightly fluorescent labeling of three subcellular compartments. A) Injection site in mouse somatosensory cortex of anterograde (locally-infecting) rabies virus encoding cytoplasmic EGFP, nuclearly-localized mTagBFP, and synaptophysin-TagRFP-T fusion protein. A tight cluster of cells primarily in layer 6 resulted from this 5 nl injection, with little labeling in more superficial layers. Descending and locally arborizing axons are brightly labeled. Overlay indicating approximate structural boundaries is adapted from Franklin and Paxinos[60]. B–D) Higher-power image of the layer 6 cells, with separate green

and blue channels showing cytoplasmic EGFP and nuclear mTagBFP. E–G) High-power image of thalamocortical axonal processes (green) and synaptic terminals (red) in primary somatosensory thalamus (ventral posteriomedial nucleus). Abbreviations: S1BF = primary somatosensory cortex, barrel field; ec = external capsule; CPu = caudate putamen. Scale bars: A 250 um, B–D 100 um, E–G 5 um.

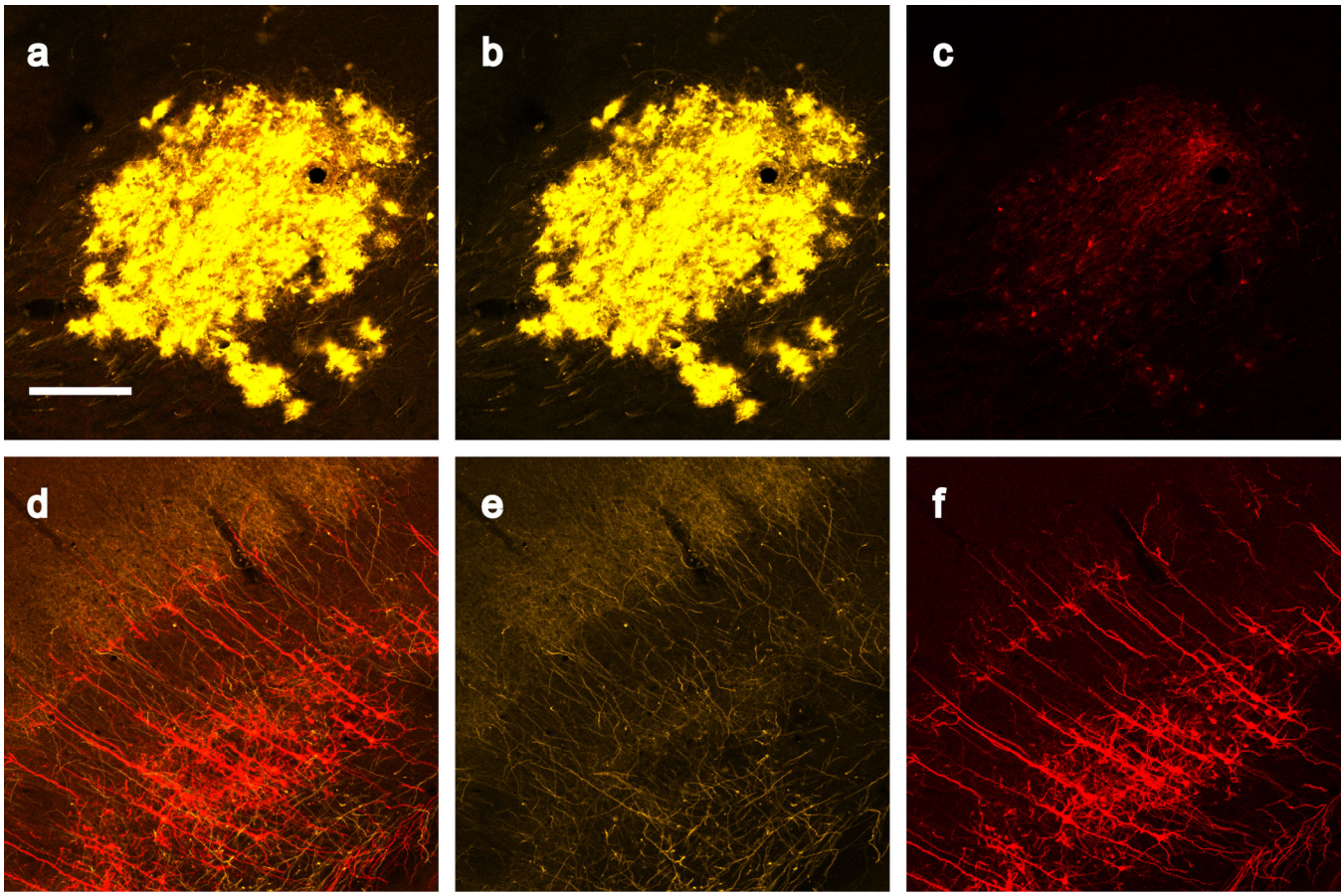

Fig. 4.

Joint retrograde and anterograde tracing of inputs and outputs of a brain region. A–C) Injection site in mouse somatosensory thalamus of an equal mixture of two deletion-mutant rabies viral vectors: an anterograde (i.e. locally-infecting) vector encoding mOrange2 (yellow), and a retrograde (i.e. infecting remote neurons projecting to the injection site) vector encoding mCherry (red). The anterograde virus prolifically infects thalamic neurons at the injection site, while the retrograde virus infects far fewer cells locally. D–F) In somatosensory cortex of the same mouse, mOrange2-filled thalamocortical axons ascend to layer 4 and densely ramify among the apical dendrites of mCherry-filled layer 6 corticothalamic cells retrogradely infected by the coinjected retrograde virus. Scale bar 200 um, applies to all panels.

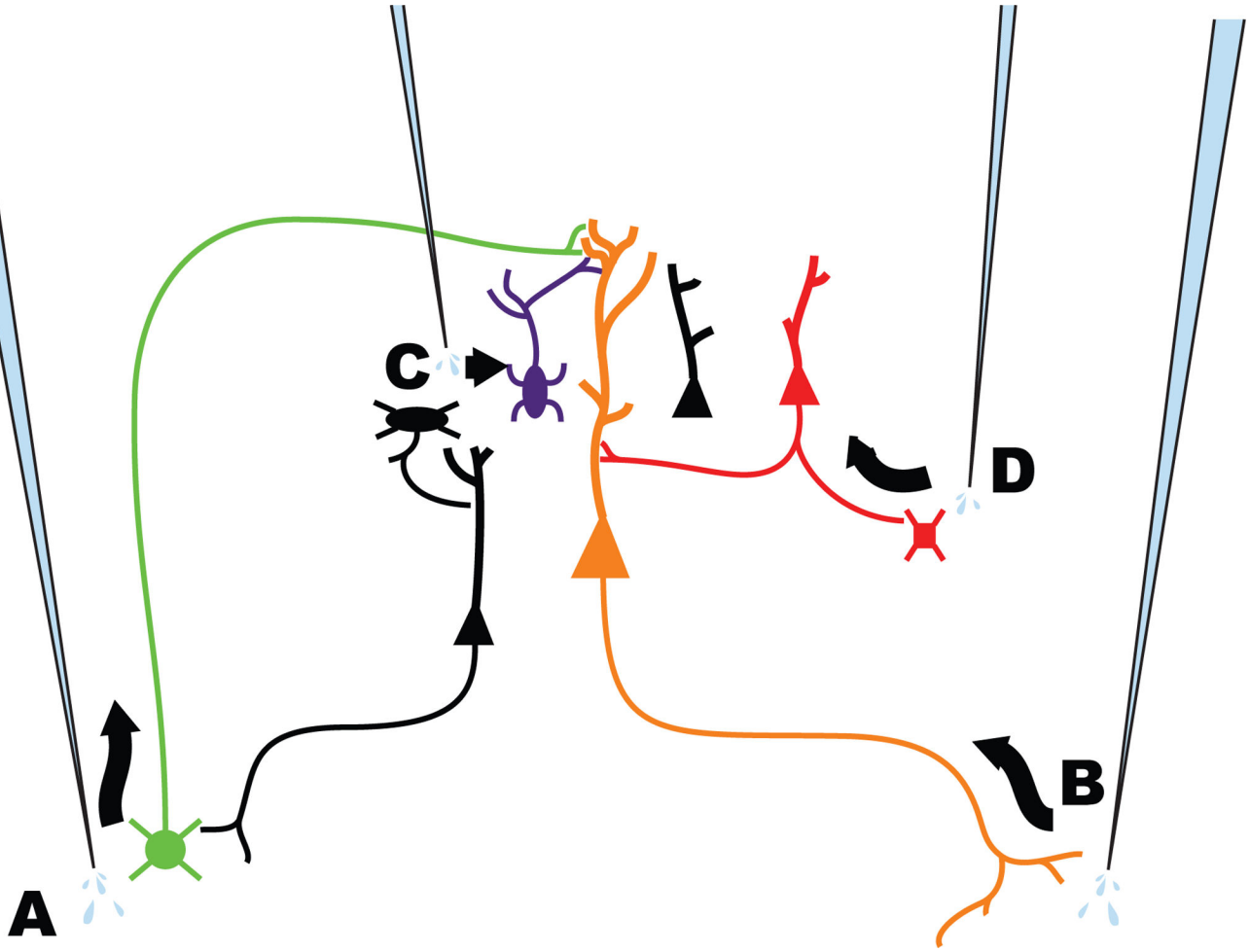

Fig. 5.

Strategies now available for targeting multiple neuronal populations with different RV vector classes. A) Anterograde targeting with VSVG-enveloped RV, introduced in this paper. B) Retrograde targeting with RVG-enveloped RV[14]. C) Genetic targeting with EnvA-enveloped RV[15]. Packaging RV with an avian retroviral envelope protein renders it unable to infect mammalian cells in the absence of engineered expression of an exogenous receptor. D) Monosynaptic targeting with RV[15]. When complemented by engineered expression of RVG *in trans*, G-deleted RV spreads to neurons directly presynaptic to the G-expressing cells.